

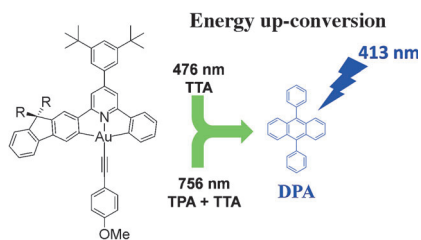
Communications



Luminescence

W.-P. To, K. T. Chan, G. S. M. Tong, C. Ma,
W.-M. Kwok, X. Guan, K.-H. Low,
C.-M. Che*      

Strongly Luminescent Gold(III)
Complexes with Long-Lived Excited
States: High Emission Quantum Yields,
Energy Up-Conversion, and Nonlinear
Optical Properties

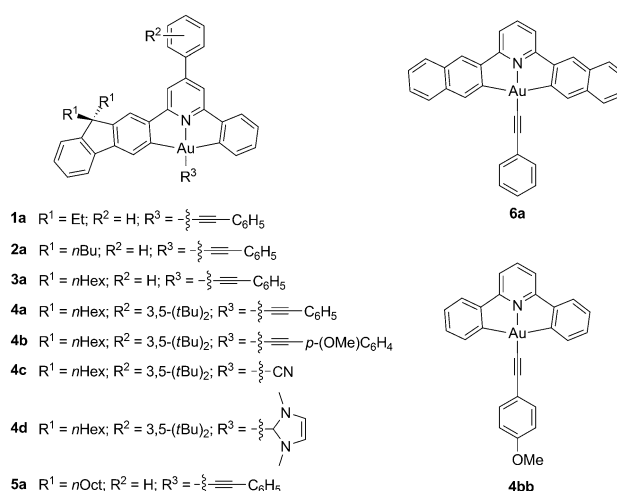


Photochemistry: A series of emissive gold(III) complexes with fluorene-containing cyclometalating ligands exhibits strong phosphorescence and long-lived excited states with emission quantum yields and lifetimes up to 58% and 305 μ s, respectively. These complexes can sensitize energy up-conversion of 9,10-diphenylanthracene (DPA; see picture) and display rich two-photon absorption properties (TPA; TTA = triplet-triplet annihilation).

Strongly Luminescent Gold(III) Complexes with Long-Lived Excited States: High Emission Quantum Yields, Energy Up-Conversion, and Nonlinear Optical Properties**

Wai-Pong To, Kaai Tung Chan, Glenna So Ming Tong, Chensheng Ma, Wai-Ming Kwok, Xiangguo Guan, Kam-Hung Low, and Chi-Ming Che*

Long-lived, strongly emissive triplet excited states such as that of the Tb^{III} complex of N^I,N^I,N^I,N^I-(ethane-1,2-diylbis(azanetriyl))tetrakis(ethane-2,1-diyl)tetrakis(2-hydroxy-N³-methylisophthalamide) and Pd^{II} porphyrins^[1] can have profound impact in diverse areas including photocatalysis^[2] and optical imaging.^[3] Triplet excited states of transition-metal complexes with lifetimes of over hundreds of microseconds usually have little metal character as the latter facilitates radiative decay through a spin-orbit coupling mechanism. In this context, luminescent Au^{III} complexes are promising systems as Au^{III} ion usually contributes little to the emissive triplet excited states. As up to now, research on luminescent gold(III) complexes is in its infancy with the reported examples hardly showing emission quantum yields over 15% in solutions at room temperature.^[4,5] Herein we show that incorporation of a fluorene moiety adjacent to a C donor atom of tridentate cyclometalated C[^]N[^]C ligands (Scheme 1) changes the lowest triplet excited state of the Au^{III} complexes from intraligand charge transfer to ligand-centered π - π^* one. Such a subtle structural modification gives rise to strongly luminescent Au^{III} complexes with unprecedentedly high emission quantum yields of up to 58% and excited state lifetimes over 200 μ s in solutions at room temperature. These strongly emissive, long-lived excited states are instrumental to the observation and investigation



Scheme 1. Chemical structures of the gold complexes.

of two-photon photophysical and photochemical properties of luminescent gold(III) systems.

The structures of the gold(III) complexes **1a–6a** are shown in Scheme 1. Details for their synthesis and characterization are given in the Supporting Information. X-ray crystal structures of **2a** and **6a** have been determined.^[6] As shown in Figure 1, the Au atoms of both **2a** and **6a** adopt a distorted square-planar geometry with C–Au–C angles of 162.3(5)–162.5(1)°. The Au–C (C[^]N[^]C ligand) and Au–N distances are 2.058(3)–2.082(12) Å and 1.958(10)–2.005(2) Å, respectively, both of which are similar to those of other cyclometalated gold(III) complexes. Interestingly, the Au–C(acetylide) distance of **2a** is 1.915(11) Å, which is notably shorter than related reported Au–C(acetylide) distances.^[4a,b,5a]

In dichloromethane solutions, complexes **1a–5a** show intense absorption bands at 250–350 nm ($\epsilon = 2$ – 5×10^4 dm³ mol⁻¹ cm⁻¹) and moderately intense absorption bands at 375–440 nm ($\epsilon = 1$ – 2×10^4 dm³ mol⁻¹ cm⁻¹); **6a** exhibits intense absorption bands at 250–320 nm ($\epsilon = 2 \times 10^4$ – 1.2×10^5 dm³ mol⁻¹ cm⁻¹) and 370–410 nm ($\epsilon = 1$ – 3×10^4 dm³ mol⁻¹ cm⁻¹). These absorption bands are assigned to intraligand transitions localized on the C[^]N[^]C ligand.

All of these gold(III) complexes having a C(flourene)-donor atom display vibronic structured emissions with peak maxima at 538–546 nm and vibrational spacings of about 1300 cm⁻¹ in CH₂Cl₂ at room temperature; these emissions are assigned to metal-perturbed intraligand transitions of the C[^]N[^]C ligand (Figure 2). Their solution emission quantum

[*] Dr. W.-P. To, K. T. Chan, Dr. G. S. M. Tong, Dr. C. Ma, Dr. X. Guan, Dr. K.-H. Low, Prof. Dr. C.-M. Che
 State Key Laboratory of Synthetic Chemistry
 Institute of Molecular Functional Materials and
 Department of Chemistry, The University of Hong Kong
 Pokfulam Road, Hong Kong (China)
 E-mail: cmche@hku.hk

Prof. Dr. C.-M. Che
 HKU Shenzhen Institute of Research and Innovation
 Shenzhen 518053 (China)

Dr. W.-M. Kwok
 Department of Applied Biology & Chemical Technology
 The Hong Kong Polytechnic University
 Hung Hom, Kowloon, Hong Kong (China)

[**] This work was supported by the Area of Excellence Scheme (grant number AoE/P-03/08), the National Key Basic Research Program of China (grant number 2013CB834802) and the CAS-Croucher Foundation Funding Scheme for Joint Laboratories, and in part using the HKU Information Technology Services research computing facilities supported by the Hong Kong UGC Special Equipment Grant (SEG HKU09).

Supporting information for this article is available on the WWW under <http://dx.doi.org/10.1002/anie.201301149>.

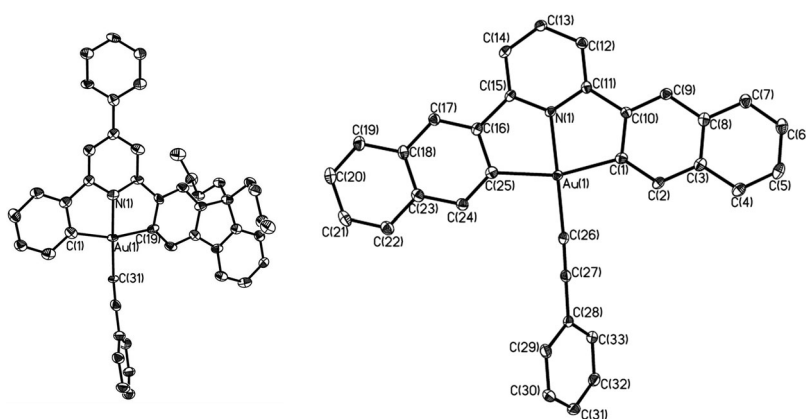


Figure 1. ORTEP representations of **2a** (left) and **6a** (right) with ellipsoids set at 35% probability. Hydrogen atoms and solvent molecules are omitted for clarity.

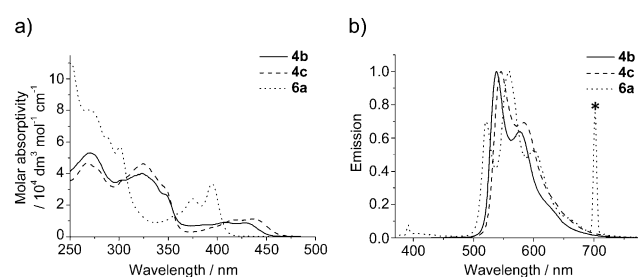


Figure 2. a) UV/Vis absorption spectra of **4b**, **4c**, and **6a** in dichloromethane. b) Emission spectra of **4b**, **4c**, and **6a** in degassed dichloromethane solutions (1×10^{-5} mol dm $^{-3}$) at room temperature. The asterisk indicates a second-order transmission of the 350 nm excitation.

yields are in most cases over 0.40 and up to 0.58, which is unprecedented in the reported luminescent gold(III) complexes. Besides the commonly encountered acetylide and N-heterocyclic carbene ligands, cyanide ligand is also effective to switch on the intraligand state (^3IL) emission of cyclo-metalated Au $^{\text{III}}$ complexes and in this work, an emission quantum yield of 0.40 for **4c** is observed. The solvent effect on the emission of **4b** has been examined. Both the emission quantum yield and lifetime of **4b** in THF ($\Phi = 0.58$, $\tau = 259$ μs) are similar to those values in CH_2Cl_2 , but these values mildly decrease when the solvent is changed to CH_3CN ($\Phi = 0.42$, $\tau = 204$ μs) and MeOH ($\Phi = 0.37$, $\tau = 193$ μs). The self-quenching rate constants for the emissions of **1a–5a** and **4b–4d** (5.0×10^6 – 8.7×10^7 mol dm $^{-3}$ s $^{-1}$) are significantly lower than that of **6a** (1.7×10^9 mol dm $^{-3}$ s $^{-1}$) presumably the dialkylfluorene moiety on the C $^{\wedge}$ N $^{\wedge}$ C ligand strongly disfavors intermolecular close contact of the gold complexes.

The simultaneous high emission quantum yields (Φ_{em} up to 58%) and long emission lifetimes (τ_0 up to 305 μs) of these Au $^{\text{III}}$ complexes are striking. Indeed, the emission quantum yields of **1a–5a** and **4b–4c** are more than 100-folds higher than the related Au(C $^{\wedge}$ N $^{\wedge}$ C) complexes reported in literature.^[5a] Femtosecond time-resolved emission measurements (350 nm excitation) with dichloromethane solutions of **4b**, **6a**, and a closely related Au $^{\text{III}}$ complex **4bb** revealed (see the Supporting Information) a very rapid decay of the S $_1$

fluorescence with the fluorescence lifetime determined to be about 0.58 ps for **4b** ($\lambda_{\text{max}} \approx 465$ nm), about 0.52 ps for **6a** ($\lambda_{\text{max}} \approx 425$ nm), and about 0.15 ps for **4bb** ($\lambda_{\text{max}} \approx 430$ nm). The sub-picosecond fluorescence decay is indicative of the presence of extremely fast nonradiative deactivation of the S $_1$ state which we attribute to intersystem crossing (ISC) from the singlet to triplet manifold with nearly unitary quantum efficiency ($\Phi_{\text{isc}} \approx 1.0$).^[4c] With this, the phosphorescence quantum yields of the complexes investigated are determined solely by the nature and dynamic competition between the radiative (k_r) versus the nonradiative (k_{nr}) decay of the emitting triplet excited states. The values of k_r and k_{nr} which were derived from the measured Φ_{em} and τ_0 are listed in Table 1. It is clear that the core cause for the remarkably high Φ_{em} and the exceptionally long τ_0 of the Au $^{\text{III}}$

Table 1: Emission data of the Au $^{\text{III}}$ complexes.

Complex	λ_{max} [nm] (τ_0 [μs]) ^[a]	Φ_{em} ^[b]	k_r [10^3 s $^{-1}$] ^[c]	k_{nr} [10^3 s $^{-1}$] ^[d]
1a	540, 580 (182)	0.43	2.4	3.1
2a	540, 579 (207)	0.44	2.1	2.7
3a	540, 578 (201)	0.51	2.5	2.4
4a	539, 579 (233)	0.55	2.4	1.9
4b	538, 579 (242)	0.58	2.4	1.7
4c	546, 583 (305)	0.40	1.3	2.0
4d	545, 583 (120)	0.13	1.1	7.3
5a	540, 579 (244)	0.45	1.8	2.3
6a	404, 521, 560 (143)	0.05	0.35	6.6

[a] Phosphorescence lifetime. [b] Phosphorescence quantum yield measured at 1×10^{-5} mol dm $^{-3}$ at room temperature using [Ru(bpy) $_3$][PF $_6$] $_2$ as standard. [c] Radiative decay rate constant estimated by $k_r = \Phi/\tau$. [d] Nonradiative decay rate constant estimated by $k_{\text{nr}} = (1 - \Phi)/\tau$.

complexes (**1a–4a**, **4b**, **4c**, and **5a**) is their low k_r (≈ 1.3 – 2.5×10^3 s $^{-1}$) combined with a similarly low or even lower k_{nr} (≈ 1.7 – 3.1×10^3 s $^{-1}$), a trait which is unique when compared to the luminescent Au $^{\text{III}}$ complexes in literature. The somewhat lower/shorter Φ_{em}/τ_0 displayed by **4d** and **6a** is due to modestly reduced k_r (≈ 0.4 – 1.1×10^3 s $^{-1}$) and a slight increase in k_{nr} (≈ 6.6 – 7.3×10^3 s $^{-1}$). On the other hand, the markedly lower/shorter Φ_{em}/τ_0 of the reported parental **4bb** (in this work: $\Phi_{\text{em}} = 0.0004$; $\tau_0 = 0.017$ μs ; $k_r = 2.35 \times 10^4$ s $^{-1}$; $k_{\text{nr}} = 5.9 \times 10^7$ s $^{-1}$) is obviously a result of its much faster k_{nr} , though its greater k_r also contributes. The drastic difference between **4b** and **4bb** in terms of k_r and especially k_{nr} implies that the triplet states of these two apparently similar complexes feature distinctively different electronic and/or structural characters. This is substantiated by DFT and TDDFT calculations revealing that the emitting triplet of **4b** is the C $^{\wedge}$ N $^{\wedge}$ C centered $\pi\pi^*$ state whereas that of **4bb** is the ligand-to-ligand charge-transfer (LLCT) state in parentage. Thus in contrast to **4b** with its triplet and S $_0$ states having similar structures and thus slow k_{nr} , **4bb** possesses a low-lying

and structurally highly distorted triplet state which serves to promote effective nonradiative decay (to S_0) thereby leading to very large k_{nr} .

DFT/TDDFT calculations performed on **4b** and **4bb** showed that, for both complexes, their HOMOs are mainly localized on the phenylacetylide ligand, and in each case the H-1 (second highest occupied molecular orbital) is a π -(C^{^N^A}C) orbital and the LUMO is predominantly a π^* -(C^{^N^A}C) orbital in character (see the Supporting Information for the MOs). When one of the phenyl rings of the C^{^N^A}C cyclometalated ligand is replaced by a fluorenyl ring, the separations between HOMO and H-1 orbitals at the ground state geometry decrease from 0.64 eV (**4bb**, benzene) to 0.20 eV (**4b**, fluorene). This is attributed to the more conjugated fluorene leading to destabilization of the π -(C^{^N^A}C) orbital. Thus the lowest singlet excited state, S_1 , of **4bb**, comes from a HOMO→LUMO transition and is assigned to ¹LLCT. On the other hand, the S_1 state of **4b** is made up mainly of a H-1→LUMO transition and is best described as a ¹ $\pi\pi^*$ excited state localized on the C^{^N^A}C cyclometalated ligand.

TDDFT calculations (M062X/6-311G*(SDD)) based on triplet geometries of **4b** and **4bb** gave emission wavelengths of 580 nm (**4b**) and 454 nm (**4bb-1**), respectively, which match with the experimental data (538 nm, **4b**; 473 nm, **4bb**). The lowest triplet excited state, T_1 , of **4b** is a ³ $\pi\pi^*$ excited state localized on the C^{^N^A}C cyclometalated ligand with an optimized geometry similar to that of S_0 (Figure 3). The highly similar geometries of the T_1 and S_0 states means that the nonradiative decay rate constant (k_{nr}) of T_1 to S_0 has to be small. For **4bb** in the ground state (S_0), as the phenylacetylide ligand can be coplanar or perpendicular to the C^{^N^A}C ligand, two forms of **4bb** were optimized as **4bb-1** (coplanar) and **4bb-2** (perpendicular), respectively.^[5a] **4bb-1** is only 0.1 kcal mol⁻¹ more stable than **4bb-2**. Starting from S_0 of **4bb-1**, optimization of the triplet state gave a coplanar structure with its emission originating from the ³LLCT excited state. The geometrical difference between T_1 and S_0 states of **4bb-1** is small, which means that the nonradiative decay rate constant (k_{nr}) of T_1 to S_0 in **4bb-1** is slow. However in the case of **4bb-2** which is just 0.1 kcal mol⁻¹ higher than **4bb-1**, the optimized T_1 of **4bb-2** was found to be 5.3 kcal mol⁻¹ more stable than the above optimized T_1 of **4bb-1** having a coplanar structure. Population of electron density into the $d\sigma^*$ orbital of Au–C^{^N^A}C in its T_1 results in a highly distorted geometry with a dihedral angle of 20.6° between Au–C1 and N–C2, and with the bond lengths of Au–C(C^{^N^A}C) and Au–N(C^{^N^A}C) substantially increased to 2.194 and 2.215 Å, respectively (see Figure 3). Such dramatic excited-state structural distortion provides a fast channel for nonradiative decay, accounting for the very low emission quantum yield (4×10^{-4}) of **4bb**.

In view of their high emission quantum yields and long excited-state lifetimes, we have examined the capacity of the present Au^{III} complexes to sensitize triplet–triplet annihilation (TTA).^[7,8] Excitation (355 nm, Nd:YAG laser) of a mixture of **4b** (2×10^{-5} mol dm⁻³) and 9,10-diphenylanthracene (DPA, 5×10^{-5} mol dm⁻³) in deoxygenated dichloromethane resulted in the observation of both prompt and delayed fluorescence of DPA and residual phosphorescence of **4b**

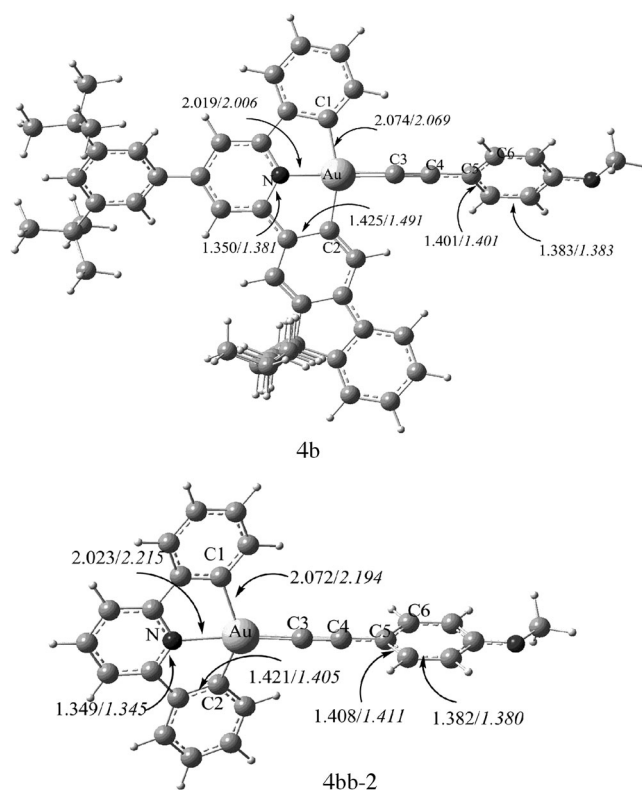


Figure 3. Comparison of the changes of key geometrical parameters of triplet state (T_1) with respect to the corresponding ground state (S_0 ; ground states in regular fonts, triplet states in italic fonts). **4b**: C3–C4 = 1.222/1.222, C4–C5 = 1.425/1.426, N–Au–C3 = 179.5/179.6, Au–C1–N–C2 = 0.1/0.1, C1–Au–C5–C6 = 50.7/52.9 and **4bb-2**: C3–C4 = 1.221/1.232, C4–C5 = 1.426/1.416, N–Au–C3 = 180.0/179.6, Au–C1–N–C2 = 0.0/20.6, C1–Au–C5–C6 = –90.0/–99.5.

(Figure 4). Excitation of either **4b** or DPA alone under the same conditions did not invoke any delayed fluorescence. Quenching experiments revealed that the rate constant of quenching of **4b*** by DPA is 1.87×10^9 dm³ mol⁻¹ s⁻¹ revealing an efficient energy transfer from **4b*** to DPA. The delayed fluorescence intensity of DPA showed a quadratic dependence ($y = x^2$) on the excitation laser power density (W cm⁻²), confirming that the delayed fluorescence is generated by a two-photon process (see the Supporting Information).^[7] To achieve up-conversion by means of TTA, we employed laser light at 476 nm to selectively excite the sensitizer and measured the fluorescence of DPA generated. As shown in Figure 4b, excitation of a mixture of sensitizer and DPA by a laser at 476 nm generated the fluorescence of DPA with complete quenching of the phosphorescence of the sensitizers. The up-conversion quantum yields were estimated to be 3.5–9.8% (Table 2).

In the literature, the main strategies used to construct molecules with large two-photon absorption (TPA) cross-sections are to increase the conjugation of the chromophore and to incorporate donor and acceptor moieties so as to create a large dipole moment.^[9] Without undertaking the aforementioned structural modification, some of the present Au^{III} complexes could give the green 538–540 nm emission (clearly visible to the naked eye, Figure 5) by excitation with

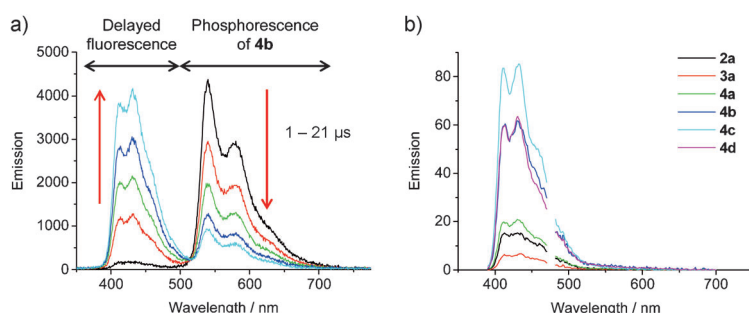


Figure 4. a) Time-resolved emission spectra of a mixture of **4b** ($2 \times 10^{-5} \text{ mol dm}^{-3}$) and DPA ($5 \times 10^{-5} \text{ mol dm}^{-3}$) in degassed dichloromethane recorded from 1 to 21 μs after laser pulse excitation (355 nm). The red arrows indicate the change in emission intensity. b) Emission spectra of mixtures of DPA ($5 \times 10^{-4} \text{ mol dm}^{-3}$) and different sensitizers ($2 \times 10^{-4} \text{ mol dm}^{-3}$) in degassed dichloromethane using 476 nm laser light for excitation. Data from 471 to 481 nm were not recorded because of the strong scattering of the laser.

Table 2: Up-conversion and two-photon absorption data for selected complexes.

Complex	$\Phi_{\text{UC}} [\%]^{\text{[a]}}$	$\sigma_2 [\text{GM}]^{\text{[b]}}$	Power dependence ^[c]
2a	4.9	7.4	1.89
3a	3.5	7.8	1.87
4a	5.9	3.4	2.09
4b	9.8	9.4	1.87
4c	7.9	3.5	–
4d	5.7	4.4	–

[a] Up-conversion quantum yield in dichloromethane using 4-(dicyanomethylene)-2-methyl-6-(4-dimethylaminostyryl)-4H-pyran as standard ($\Phi = 0.10$ in dichloromethane).^[8d] [b] Two-photon absorption cross-section determined using fluorescein as standard. [c] Slope of the double-log plot of the emission intensity induced by two-photon absorption against the excitation power density.

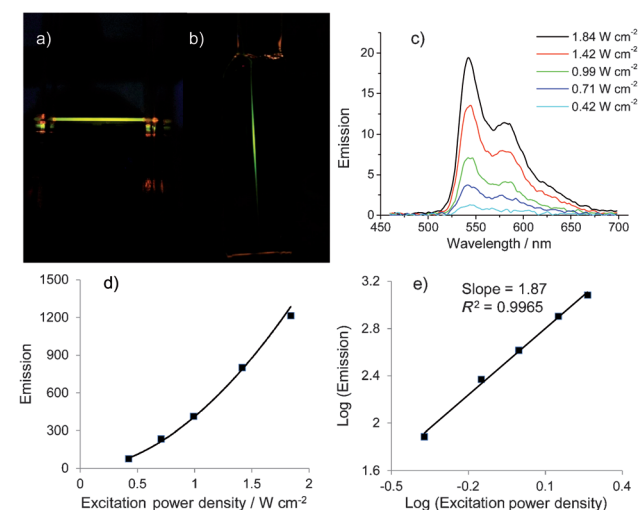


Figure 5. Emission of **4b** ($2 \times 10^{-4} \text{ mol dm}^{-3}$) in dichloromethane excited with 756 nm laser light. a and b) Photos showing the emission of solution. c) Emission spectra using different excitation power densities. d) Plot of emission intensity against excitation power density (W cm^{-2}). e) Double-log plot of emission intensity against excitation power density.

a focused 756 nm laser beam, the spectra of which are the same as their corresponding emission spectra obtained by excitation with a xenon lamp at 400–430 nm. As all of these complexes do not show any linear absorption at 756 nm, the emission generated by excitation at 756 nm can be attributed to TPA-induced emission. The two-photon absorption cross sections (σ_2) were estimated to be 3.4–9.4 GM (Table 2) by the literature method with fluorescein as reference.^[10]

As shown in Figure 5, the emission intensity of **4b** displays a quadratic dependence ($y = x^2$) on the laser power density, confirming that two light photons at 756 nm are required for one emitted photon. As **4b** could sensitize TTA and displays TPA properties, **4b** was used to generate the fluorescence of DPA by a TTA process.^[11] When a deoxygenated solution of **4b** and DPA in dichloromethane was brought to the focus point of the 756 nm laser beam, a blue line with an emission spectrum identical to the fluorescence spectrum of DPA has been recorded (Figure 6). Control experiment revealed that this blue line emission can be observed only when **4b** is present. Importantly, a remarkably high anti-Stokes shift of 1.36 eV (756 \rightarrow 413 nm) can be achieved by combining TPA and TTA. The emission intensity of DPA caused by TPA-induced TTA was reported to display a quartic ($y = x^4$) incident light power

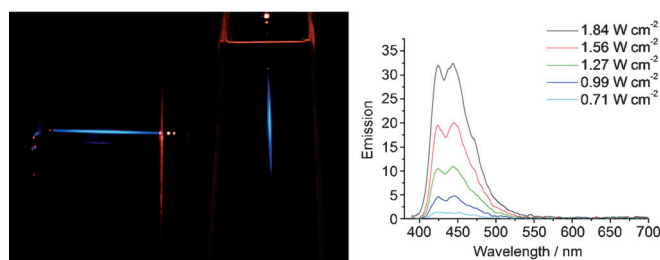
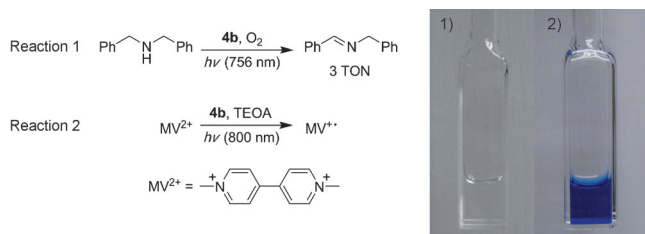


Figure 6. Emission of a mixture of **4b** ($2 \times 10^{-4} \text{ mol dm}^{-3}$) and DPA ($5 \times 10^{-4} \text{ mol dm}^{-3}$) in dichloromethane induced by two-photon absorption excited with 756 nm laser light. Left: Photos showing the emission of a mixture of **4b** ($2 \times 10^{-4} \text{ mol dm}^{-3}$) and DPA ($5 \times 10^{-4} \text{ mol dm}^{-3}$) in degassed dichloromethane excited with a 756 nm laser. Right: Emission spectra using different excitation power densities.

dependence.^[11] In this study, the power dependence obtained from a double-log plot of the emission intensity against the excitation power density was found to be 3.31 (i.e. $y = x^{3.31}$), suggesting that it is at least a three-photon process.

While applications of TPA in fluorescence microscopy^[12] and photodynamic therapy^[13] are well-documented, research regarding the photochemistry/photocatalysis stemming from TPA is utterly unexplored.^[14] The importance of TPA-induced photochemistry lies in the use of light radiation that is normally not absorbed by transition-metal complexes (sensitizers) ($\lambda > 700 \text{ nm}$). In our initial trials, we found that: 1) Three turnovers of imines were furnished by irradiating a mixture of **4b** and dibenzylamine with laser light at 756 nm under aerobic conditions for 2 h. 2) Formation of the methyl viologen radical cation ($\text{MV}^{+\cdot}$) was observed by irradiating

a mixture of **4b**, MV²⁺, and triethanolamine (TEOA) in degassed acetonitrile with 800 nm laser light (Scheme 2). Control experiments showed that in both cases no photochemistry could be observed in the absence of **4b**. With these preliminary results, we conceive that solar energy, which is concentrated in the near-infrared spectral region, could be harnessed for the photochemical reactions of phosphorescent



Scheme 2. Left: Photochemical reactions catalyzed by **4b** using a near-infrared laser as light source. Right: Photos showing the color of the solution of reaction 2 in 1) the absence and 2) presence of **4b** after irradiation by 800 nm laser light for 30 minutes (MV²⁺ = methyl viologen dication).

gold(III) complexes that do not absorb strongly in the visible to near-infrared spectral region.

In conclusion, a series of metal–organic gold(III) complexes which display unprecedentedly high emission quantum yields and long-lived excited states have been synthesized. We have also described, for the first time, the TTA and TPA properties of metal–organic gold(III) complexes and the use of TPA for photoinduced oxidation and electron-transfer reactions.

Received: February 8, 2013

Revised: April 22, 2013

Published online: ■ ■ ■ ■ ■, ■ ■ ■ ■ ■

Keywords: energy up-conversion · gold · luminescence · photochemistry · two-photon absorption

- [1] a) A. Y. Lebedev, M. A. Filatov, A. V. Cheprakov, S. A. Vinogradov, *J. Phys. Chem. A* **2008**, *112*, 7723–7733; b) E. G. Moore, A. P. S. Samuel, K. N. Raymond, *Acc. Chem. Res.* **2009**, *42*, 542–552.
- [2] a) T. S. Teets, D. G. Nocera, *Chem. Commun.* **2011**, *47*, 9268–9274; b) W. T. Eckenhoff, R. Eisenberg, *Dalton Trans.* **2012**, *41*, 13004–13021; c) J. W. Tucker, C. R. J. Stephenson, *J. Org. Chem.* **2012**, *77*, 1617–1622; d) L. Shi, W. Xia, *Chem. Soc. Rev.* **2012**, *41*, 7687–7697.
- [3] a) K. K.-W. Lo, M.-W. Louie, K. Y. Zhang, *Coord. Chem. Rev.* **2010**, *254*, 2603–2622; b) K. K.-W. Lo, K. Y. Zhang, *RSC Adv.* **2012**, *2*, 12069–12083; c) F. L. Thorp-Greenwood, *Organometallics* **2012**, *31*, 5686–5692; d) E. Baggailey, J. A. Weinstein, J. A. G. Williams, *Coord. Chem. Rev.* **2012**, *256*, 1762–1785.
- [4] a) V. K.-M. Au, K. M.-C. Wong, N. Zhu, V. W.-W. Yam, *Chem. Eur. J.* **2011**, *17*, 130–142; b) J. A. Garg, O. Blacque, K. Venkatesan, *Inorg. Chem.* **2011**, *50*, 5430–5441; c) W.-P. To, G. S.-M. Tong, W. Lu, C. Ma, J. Liu, A. L.-F. Chow, C.-M. Che, *Angew. Chem. Int. Ed.* **2012**, *51*, 2654–2657; d) D. A. Smith, D.-A. Roşca, M. Bochmann, *Organometallics* **2012**, *31*, 5998–6000; e) D.-A. Roşca, D. A. Smith, M. Bochmann, *Chem. Commun.* **2012**, *48*, 7247–7249.
- [5] a) K. M.-C. Wong, L.-L. Hung, W. H. Lam, N. Zhu, V. W.-W. Yam, *J. Am. Chem. Soc.* **2007**, *129*, 4350–4365; b) V. K.-M. Au, K. M.-C. Wong, N. Zhu, V. W.-W. Yam, *J. Am. Chem. Soc.* **2009**, *131*, 9076–9085; c) J. A. Garg, O. Blacque, T. Fox, K. Venkatesan, *Inorg. Chem.* **2010**, *49*, 11463–11472; d) C. Bronner, O. S. Wenger, *Dalton Trans.* **2011**, *40*, 12409–12420; e) V. K.-M. Au, N. Zhu, V. W.-W. Yam, *Inorg. Chem.* **2013**, *52*, 558–567.
- [6] CCDC 919888 (**6a**) and 919889 (**2a**) contain the supplementary crystallographic data for this paper. These data can be obtained free of charge from The Cambridge Crystallographic Data Centre via www.ccdc.cam.ac.uk/data_request/cif.
- [7] a) T. N. Singh-Rachford, F. N. Castellano, *Coord. Chem. Rev.* **2010**, *254*, 2560–2573; b) J. Zhao, S. Ji, W. Wu, W. Wu, H. Guo, J. Sun, H. Sun, Y. Liu, Q. Li, L. Huang, *RSC Adv.* **2012**, *2*, 1712–1728.
- [8] Selected articles on TTA-based up-conversion: a) D. V. Kozlov, F. N. Castellano, *Chem. Commun.* **2004**, 2860–2861; b) R. R. Islangulov, J. Lott, C. Weder, F. N. Castellano, *J. Am. Chem. Soc.* **2007**, *129*, 12652–12653; c) P. Du, R. Eisenberg, *Chem. Sci.* **2010**, *1*, 502–506; d) S. Ji, W. Wu, W. Wu, H. Guo, J. Zhao, *Angew. Chem. Int. Ed.* **2011**, *50*, 1626–1629; e) H. Guo, Q. Li, L. Ma, J. Zhao, *J. Mater. Chem.* **2012**, *22*, 15757–15768.
- [9] a) G. S. He, L.-S. Tan, Q. Zheng, P. N. Prasad, *Chem. Rev.* **2008**, *108*, 1245–1330; b) M. Pawlicki, H. A. Collins, R. G. Denning, H. L. Anderson, *Angew. Chem.* **2009**, *121*, 3292–3316; *Angew. Chem. Int. Ed.* **2009**, *48*, 3244–3266.
- [10] M. A. Albota, C. Xu, W. W. Webb, *Appl. Opt.* **1998**, *37*, 7352–7356.
- [11] T. N. Singh-Rachford, F. N. Castellano, *J. Phys. Chem. A* **2009**, *113*, 9266–9269.
- [12] a) J. W. Grate in *Reviews in Fluorescence, Vol. 2007* (Ed.: C. D. Geddes), Springer, New York, **2009**, pp. 249–269; b) N. A. A. Rahim, W. McDaniel, K. Bardson, S. Srinivasan, V. Vickerman, P. T. C. So, J. H. Moon, *Adv. Mater.* **2009**, *21*, 3492–3496; c) A. Parthasarathy, H.-Y. Ahn, K. D. Belfield, K. S. Schanze, *ACS Appl. Mater. Interfaces* **2010**, *2*, 2744–2748; d) S. Sumalekshmy, C. J. Fahrni, *Chem. Mater.* **2011**, *23*, 483–500.
- [13] a) J. R. Starkey, A. K. Rebane, M. A. Drobizhev, F. Meng, A. Gong, A. Elliott, K. McInnerney, C. W. Spangler, *Clin. Cancer Res.* **2008**, *14*, 6564–6573; b) M. Velusamy, J.-Y. Shen, J. T. Lin, Y.-C. Lin, C.-C. Hsieh, C.-H. Lai, C.-W. Lai, M.-L. Ho, Y.-C. Chen, P.-T. Chou, J.-K. Hsiao, *Adv. Funct. Mater.* **2009**, *19*, 2388–2397; c) X. Shen, F. He, J. Wu, G. Q. Xu, S. Q. Yao, Q.-H. Xu, *Langmuir* **2011**, *27*, 1739–1744; d) L. T. Bergendahl, M. J. Paterson, *J. Phys. Chem. B* **2012**, *116*, 11818–11828.
- [14] Y. Zhao, G. M. Roberts, S. E. Greenough, N. J. Farrer, M. J. Paterson, W. H. Powell, V. G. Stavros, P. J. Sadler, *Angew. Chem. Int. Ed.* **2012**, *51*, 11263–11266.